The Canadian Mineralogist
Vol. 35, pp. 1221-1236 (1997)

PETROLOGY OF THE FLINTON CREEK METAPERIDOTITES: ENSTATITE – MAGNESITE AND ANTHOPHYLLITE – MAGNESITE ASSEMBLAGES FROM THE GRENVILLE PROVINCE

FREDERICK D. FORD* AND GEORGE B. SKIPPEN

Ottawa – Carleton Geoscience Center, Department of Geology, Carleton University, Ottawa, Ontario K1S 5B6

ABSTRACT

Two types of metaperidotite, enstatite – magnesite rock and anthophyllite – magnesite – dolomite rock, are present in ultramafic lenses from the southern Flinton Synclinorium, Central Metasedimentary Belt, Grenville Province, in southeastern Ontario. A mantle of the anthophyllite – carbonate rock always surrounds the primary enstatite – magnesite rock, which is preserved only in the interior of the larger ultramafic lenses. The enstatite – magnesite rock contains enstatite (Mg_{90}), magnesite (Mg_{94}), dolomite (Mg_{49}), as well as talc (Mg_{97}), anthophyllite (Mg_{88}), forsterite (Mg_{90}), and relict chromian magnetite. The assemblage enstatite + magnesite requires the presence of a relatively CO_2-rich fluid phase. The presence of late-stage forsterite veins in the enstatite – magnesite rock may be explained by infiltration of comparatively H_2O-rich fluid at near-thermal-peak metamorphic conditions. The anthophyllite – carbonate rock is composed of spherically radiating anthophyllite intergrown with magnesite, dolomite and chromian magnetite; the compositions of minerals are similar in the two rock types. The presence of only one silicate in addition to the carbonates suggests that the anthophyllite – carbonate assemblage formed as a metasomatic mantle during the early retrograde history of the ultramafic lenses. Kyanite – biotite assemblages in adjacent pelitic rocks indicate a regional metamorphic grade in the middle amphibolite facies. Thermobarometry records metamorphic temperatures of 620° to 680°C at pressures of 6.5 to 7.5 kbar.

Keywords: metaperidotite, ultramafic, anthophyllite, enstatite, magnesite, Grenville Province, Flinton Group, Ontario.

SOMMAIRE

Nous décrivons deux sortes de métapéridotite, soit une roche à enstatite + magnésite et une autre à anthophyllite + magnésite + dolomite, dans des lentilles ultramafiques affleurant dans le synclinorium de Flinton, de la ceinture métasédimentaire centrale de la Province du Grenville, au sud-est de l'Ontario. Un liseré à anthophyllite + carbonate entoure dans tous les cas la roche primaire à enstatite + magnésite, préservée seulement à l'intérieur des plus grosses lentilles ultramafiques. La roche à enstatite + magnésite contient enstatite (Mg_{90}), magnésite (Mg_{94}), dolomite (Mg_{49}), de même que talc (Mg_{97}), anthophyllite (Mg_{88}), forstérite (Mg_{90}), et magnétite chromifère résiduelle. L'assemblage enstatite + magnésite implique la présence d'une phase fluide relativement riche en CO_2. La présence de veines tardives à forstérite dans la roche à enstatite + magnésite résulterait peut-être de l'infiltration d'une phase fluide comparativement plus riche en H_2O à des conditions de température proches de celles du paroxysme métamorphique. La roche à anthophyllite + carbonate contient des cristaux d'anthophyllite fibroradiés en intercroissance avec magnésite, dolomite et magnétite chromifère. Les compositions des minéraux sont semblables dans les deux sortes de roche. Vu la présence d'un seul silicate avec ces carbonates, l'association anthophyllite + carbonate représenterait un liseré métasomatique formé lors de la rétrogression précoce de ces lentilles. Les assemblages à kyanite + biotite des roches pélitiques adjacentes indiquent un degré de métamorphisme régional dans le faciès amphibolite moyen. La thermobarométrie indique une température de métamorphisme de 620° à 680°C à une pression entre 6.5 et 7.5 kbar.

(Traduit par la Rédaction)

Mots-clés: métapéridotite, ultramafique, anthophyllite, enstatite, magnésite, Province du Grenville, Groupe de Flinton, Ontario.

INTRODUCTION

Metaperidotitic rocks are exposed in a series of discontinuous boudins along the eastern margin of the Flinton Synclinorium, located in the Central Metasedimentary Belt (Wynne-Edwards 1972) of the Grenville Structural Province, in southeastern Ontario (Fig. 1). The ultramafic boudins, herein termed the Flinton Creek Metaperidotites, are associated with a suite of metamorphosed mafic rocks ranging from metagabbro to amphibolite. The metaperidotites are interesting in that they contain significant proportions

* Present address: Geoscience Laboratories, 933 Ramsey Lake Road, Sudbury, Ontario P3E 6B5.
E-mail address: ford_f@torv05.ndm.gov.on.ca

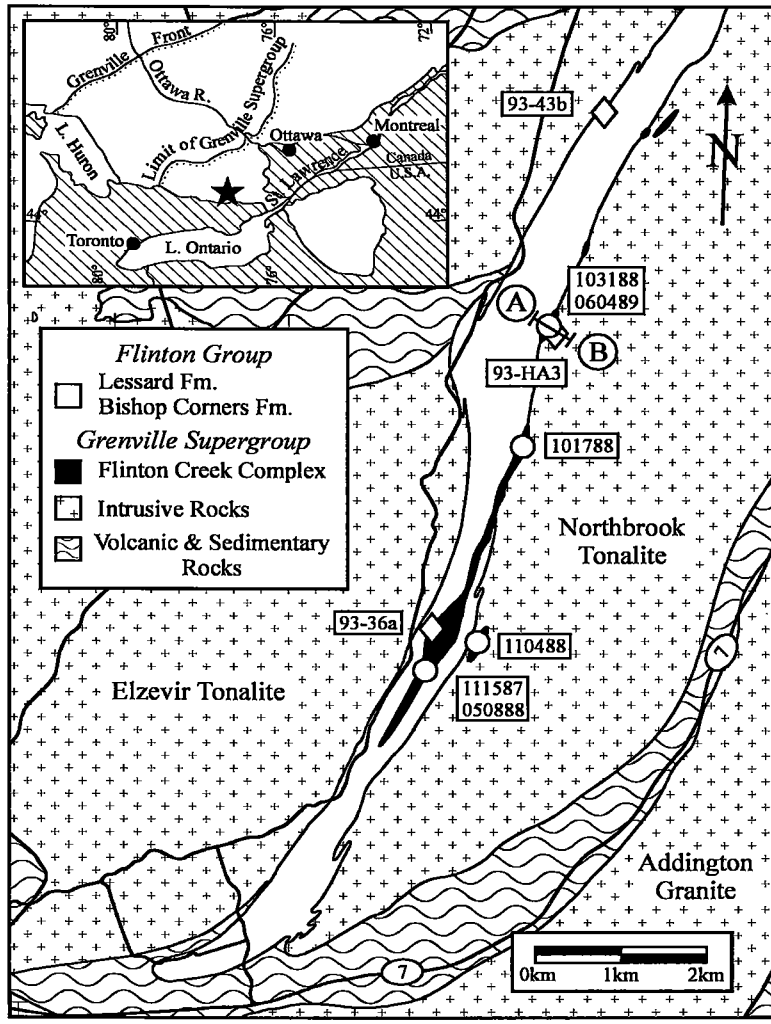

FIG. 1. Geology of the southern Flinton Synclinorium and surrounding area; asterisk in inset map indicates geographic location. Open dots show the location of samples of ultramafic rock mentioned in the text. Diamonds indicate location of samples used for thermobarometry. The main body of the Flinton Creek Complex (black) occurs within the Flinton Group, in the core of the synclinorium, with a long tail extending northward to the contact with the Northbrook Tonalite. Sporadic lenses of ultramafic rocks occur north of this point, in the contact zone between the tonalite and the Flinton Group. At least two ultramafic lenses occur entirely within the Northbrook, several hundred meters away from the contact (sample 110488). The Flinton Synclinorium is bounded on the east and west sides by shear zones that have not been indicated. The compilation was produced from the observations of Thompson (1972), Chappell (1978), and Bright (1986).

of magnesite and dolomite, in addition to silicate minerals more commonly associated with metamorphosed ultramafic rocks, such as enstatite, anthophyllite, tremolite and forsterite (Trommsdorff & Evans 1974). In this paper, we discuss the petrology of these carbonate-bearing ultramafic rocks and describe their petrogenesis on the basis of observed assemblages and textures of the minerals, thermobarometry, and calculated phase-relations.

Field Relations

The metaperidotites generally occur as lenses in an elongate belt of deformed mafic rocks. Together, the mafic and ultramafic rocks form what is herein termed the Flinton Creek Complex. Individual ultramafic lenses vary in size from 1 m to over 50 m in longest dimension. Larger lenses contain a core of enstatite – magnesite rock surrounded by an envelope of

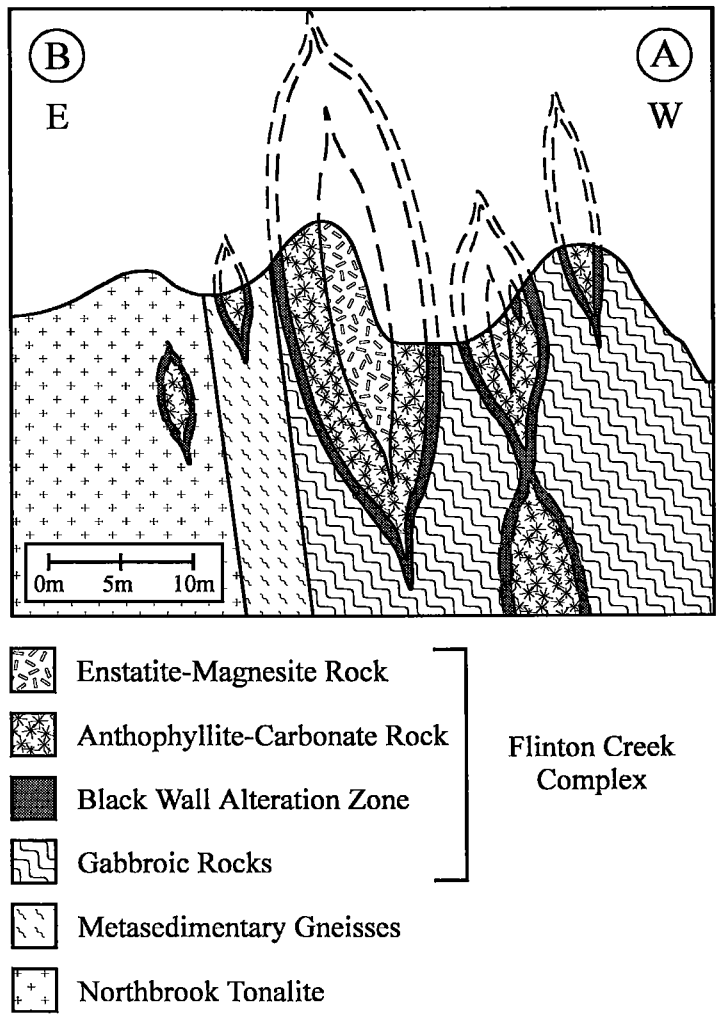

FIG. 2. Hypothetical cross-section of several ultramafic lenses looking along strike. Foliation in the host rock is subparallel to the long axis of the ultramafic lenses as drawn; however, the direction of maximum elongation is perpendicular to the diagram. Note that the two ultramafic rock-types form concentric zones, with enstatite – magnesite rock in the core of the larger lenses, surrounded by an envelope of anthophyllite – carbonate rock. Smaller ultramafic lenses consist entirely of the anthophyllite – carbonate assemblage.

anthophyllite – carbonate rock. Smaller lenses are composed entirely of anthophyllite – carbonate rock. Sample locations are shown on Figure 1. An idealized cross-section through the Flinton Creek Complex is shown as Figure 2.

A metasomatic reaction-zone or "blackwall" 10 to 20 cm thick is developed where the ultramafic lenses are in contact with the surrounding metamorphosed mafic rocks. Similar reaction-zones have been described from other localities of metamorphosed ultramafic rocks around the world, including Paddy-Go-Easy Pass (Frost 1975) and the northern Appalachians (Jahns 1967, Sanford 1982). The following mineral zones progress outward from the ultramafic lens into the surrounding mafic rocks: monomineralic tremolite zone, monomineralic biotite zone, chlorite zone. This sequence of mineral zones is similar to the amphibolite-facies blackwall zones described by Sanford (1982) at Blandford, Massachusetts and Grafton, Vermont. The presence of this metasomatic reaction-zone between the ultramafic lenses and the surrounding host-rocks indicates that the two dissimilar rock-types were in contact with each other during regional metamorphism, eliminating the possibility of post-metamorphic tectonic emplacement for the metaperidotites.

Metamorphism

Pelitic schist from the Bishop Corners Formation, containing the assemblage kyanite + biotite + staurolite + muscovite + quartz (Ford & Skippen 1994), is coincident with the northernmost occurrence of the ultramafic rocks at locality 93–43 (Fig. 1). An increase in regional metamorphic grade southward from this locality has been demonstrated in calcareous sedimentary rocks of the Lessard Formation (Thompson 1973), indicating that the assemblage kyanite – biotite gives a minimum estimate of metamorphic grade for the Flinton Creek Complex. Mafic rocks within the Complex contain assemblages compatible with this estimate (amphibole – plagioclase – epidote – garnet). The increase in metamorphic grade southward within the Flinton Synclinorium is supported by the appearance of two-mica granitic pegmatite (with or without garnet) in Flinton Group psammitic rocks that are spatially related to the metaperidotites southward from locality 101788 on Figure 1; Thompson (1973) interpreted the bodies of granitic pegmatite to be produced by partial melting of the Flinton Group psammites.

Samples for geothermobarometry were collected from several rock-types, including: pelitic schist, garnet-bearing amphibolite, and semipelitic gneiss containing garnet, amphibole, and biotite. The stratigraphic position of this last-named rock-type is unknown, as it is exposed only intermittently between the Flinton Creek Complex and the Northbrook Tonalite. Thermobarometric results are summarized in Table 1. Temperature estimates range from 620° to 680°C. Estimated pressures are 6.5 to 7.5 kbar. Thermobarometric results for 93–43b (staurolite – kyanite – biotite) are consistent with published grids for metapelite (*e.g.*, Powell & Holland 1990), which indicate the stability of this assemblage at the estimated temperature and pressure. The thermobarometry for sample 93–43b indicates metamorphic conditions approaching the stability field of sillimanite; this is in agreement with the regional location of the kyanite-to-sillimanite isograd (Carmichael *et al.* 1978) that lies between outcrop 93–43 (staurolite – kyanite – biotite) and sillimanite-bearing pelitic schists 4 km to the east.

TABLE 1. GEOTHERMOBAROMETRY RESULTS

	Thermometry (°C)			Barometry (bars)	
	(1)	(2)	(3)	(3)	(4)
93-43b	614		616 ± 20	6400 ± 1280	
93-HA3	638	714	654 ± 7	6765 ± 155	7500
93-36a	737	685	750 ± 18	7425 ± 675	6200

(1) Garnet – biotite thermometry using the calibration of Hodges & Spear (1982) for a pressure of 7 kbar. (2) Amphibole – plagioclase thermometry using the calibration of Holland & Blundy (1994) for a pressure of 7 kbar. (3) INTERSX results using TWQ (version 1.02; Berman 1991). The ± values represent 1 σ scatter of intersections. (4) Amphibole – garnet – plagioclase barometry using the calibration of Kohn & Spear (1990) at T(1). Mineral assemblages: Grt – Bt – Ms – Ky – Pl – Qtz (93-43b), Grt – Bt – Hbl – Pl – Qtz (93-HA3, 93-36a). Mineral compositions used to obtain the P–T results are available upon request from the first author, and from the Depository of Unpublished Data, CISTI, National Research Council of Canada, Ottawa, Ontario K1A 0S2.

Petrography and Mineral Chemistry

Approximately 250 samples distributed throughout the Flinton Creek Complex were selected for detailed petrographic examination. The locations of samples investigated by electron-microprobe analysis (Tables 2, 3) are shown on Figure 1.

Whole-rock chemistry

Sixteen samples of enstatite – magnesite and anthophyllite – carbonate rock were collected for whole-rock geochemistry throughout the Flinton Creek Complex; representative compositions are given in Table 4. Low analytical totals, due to the presence of carbonates and hydrous minerals, preclude an extensive discussion of the chemical petrogenesis of these rocks; however, it is worth noting that both rock types have high levels of Cr (2000–7500 ppm) and Ni (1000–2300 ppm) contents, which is compatible with an ultramafic protolith. The proportions of Si, Fe and Mg remain within the range expected for ultramafic rocks, indicating that variations in bulk composition are not responsible for the different mineral assemblages

TABLE 2. AVERAGE COMPOSITION OF ENSTATITE, OLIVINE, ANTHOPHYLLITE AND TREMOLITE *

Sample		Enstatite			Olivine					Anthophyllite			Tremolite	
		111587-1c	110488-c2	101788-1b	111587-1c	110488-c2	101788-1b	060489-2b	050888-2a	111587-1c	110488-c2	103188-c1	111587-1c	110488-c2
		(9)	(14)	(41)	(4)	(46)	(26)	(48)	(26)	(6)	(46)	(18)	(29)	(7)
Rk. Type		EM	EM	EM	EM	EM	EM	EM	EM	EM	EM	AC	EM	EM
SiO2	wt.%	57.65	57.46	57.93	41.49	40.68	40.97	40.95	40.79	59.48	59.12	58.33	57.33	54.74
TiO2		0.07	0.10	0.11	–	–	–	–	–	0.08	0.08	0.07	0.18	0.18
Al2O3		0.08	0.00	0.14	–	–	–	–	–	0.14	0.36	0.22	0.67	2.44
Cr2O3		0.10	0.10	0.14	–	–	–	–	–	0.10	0.06	0.07	0.33	0.45
FeO		6.05	7.25	6.19	8.09	9.32	8.67	9.30	8.54	6.88	6.98	7.81	1.93	2.68
MnO		0.14	0.24	0.15	0.16	0.16	0.14	0.10	0.20	0.35	0.25	0.16	0.12	0.09
MgO		34.99	34.57	35.08	50.98	48.77	49.36	49.37	50.07	30.72	30.78	29.85	23.64	22.62
NiO		–	–	–	0.74	0.37	0.62	0.39	0.52	–	–	–	–	–
CaO		0.09	0.11	0.10	–	–	–	–	–	0.70	0.36	0.34	13.20	12.85
K2O		–	–	–	–	–	–	–	–	0.12	0.12	0.13	0.09	0.09
Total		99.17	99.83	99.84	101.46	99.30	99.76	100.11	100.11	98.57	98.11	96.98	97.49	96.14
Oxygen atoms		6	6	6	4	4	4	4	4	23	23	23	23	23
Si		1.998	1.992	1.996	0.997	1.003	1.003	1.001	0.995	7.947	7.917	7.944	7.863	7.642
Ti		0.002	0.003	0.003	–	–	–	–	–	0.008	0.008	0.007	0.018	0.019
Al		0.003	0.000	0.006	–	–	–	–	–	0.021	0.057	0.035	0.109	0.402
Cr		0.003	0.003	0.004	–	–	–	–	–	0.011	0.007	0.008	0.036	0.049
Fe		0.175	0.210	0.179	0.162	0.192	0.178	0.190	0.174	0.769	0.782	0.890	0.221	0.313
Mn		0.004	0.008	0.004	0.003	0.003	0.003	0.002	0.004	0.040	0.029	0.018	0.014	0.010
Mg		1.808	1.786	1.791	1.826	1.792	1.802	1.799	1.821	6.118	6.144	6.058	4.834	4.706
Ni		–	–	–	0.014	0.007	0.012	0.008	0.010	–	–	–	–	–
Ca		0.003	0.004	0.004	–	–	–	–	–	0.100	0.050	0.050	1.940	1.923
K		–	–	–	–	–	–	–	–	0.020	0.021	0.022	0.015	0.016
Total		3.996	4.006	3.987	3.002	2.997	2.998	3.000	3.005	15.034	15.015	15.032	15.050	15.080
mg# †		0.91	0.89	0.91	0.91	0.90	0.90	0.90	0.91	0.88	0.88	0.87	0.95	0.94

† Mg/(Fe+Mn+Mg+Ni)

* determined by electron-microprobe analysis. The number of analyses is given in brackets. Analysis on Carleton University Cambridge Microscan V electron microprobe equipped with an energy dispersive spectrometer. Operating conditions were 20KV and a specimen current of 9 namp. Average collection time was 100s live time. Data reduction was completed on a personal computer using the EDDI program of Pringle (1989).

present in the enstatite – magnesite and anthophyllite – carbonate rocks. The analytical data of Table 4 are compared with standard ultramafic compositions on Figure 3.

Petrography of the enstatite – magnesite rock

The enstatite – magnesite rock is composed primarily of coarse-grained, euhedral enstatite and medium- to fine-grained magnesite (Fig. 4a). Pettersen (1883) applied the name *sagvandite* to similar carbonate-orthopyroxenites from the Troms region of northern Norway. Carbonate-bearing orthopyroxenites have also been described from Aaheim, western Norway (Kendel 1970) and the Central Alps (Evans & Trommsdorff 1970, 1974). Additional work on the Troms locality has been presented by Schreyer *et al.* (1972) and Ohnmacht (1974). A review of Norwegian metamorphosed ultramafic rocks is provided by Bucher-Nurminen (1988).

Textures in this rock type are complex, with obvious replacement and overgrowth of early minerals complicated by the later development of vein-related minerals such as magnesite and olivine. The driving force for the development of these textures is believed to be fluid influx. As such, the concept of "local equilibrium", as defined by Thompson (1959), is believed to apply to the Flinton Creek Metaperidotites, whereby "equilibrium tends to be maintained locally within a reacting system even though the system as a whole may be distinctly out of equilibrium."

Enstatite in the enstatite – magnesite rock is coarse-grained (10 – 30 mm) and subhedral, and forms a network of mutually interfering crystals. Chlorite, opaque minerals and minor amounts of carbonate occur as randomly oriented inclusions in enstatite. Several electron-microprobe traverses across the larger grains of enstatite revealed no compositional zonation. Enstatite crystals from different localities throughout the complex have similar compositions (Table 2).

The rock is composed of 20 to 30% carbonate minerals. Magnesite commonly occurs as fine- to medium-grained, anhedral crystals in magnesite-rich domains found interstitially among, and surrounding, the coarser-grained crystals of enstatite; however, a small number of samples have large, single crystals of coarse-grained (1 – 5 cm), euhedral magnesite in textural equilibrium with the adjacent enstatite (Fig. 4a). Anhedral magnesite is commonly associated with anthophyllite. Enclaves of magnesite – anthophyllite can be found within large grains of enstatite, or on grain boundaries, where the two minerals seem to be growing into the larger crystal (Fig. 4b). The following reaction describes the relationship among the three

TABLE 3. AVERAGE COMPOSITION OF CARBONATES, TALC AND CHLORITE *

	Magnesite			Dolomite		Talc		Chlorite
Sample	111587	110488	101788	111587	110488	101788	103188	111587
	-1c	-c3	-1b	-1c	-c3	-1a	-c2	-1c
	(10)	(11)	(9)	(12)	(9)	(10)	(27)	(4)
Rk. Type	EM	EM	EM	EM	EM	EM	AC	EM
SiO2 wt. %	–	–	–	–	–	62.06	61.86	32.89
TiO2	–	–	–	–	–	0.14	0.12	0.10
Al2O3	–	–	–	–	–	0.15	1.13	16.31
Cr2O3	–	–	–	–	–	0.12	0.16	1.31
FeO	3.56	4.66	4.29	1.16	1.45	1.16	1.21	3.44
MnO	0.26	0.23	0.18	0.08	0.08	0.06	0.06	0.11
MgO	44.82	43.66	44.48	21.25	20.97	30.45	30.36	35.01
NiO	–	–	–	–	–	0.35	0.29	0.41
CaO	0.44	0.39	0.44	29.25	29.23	–	–	–
K2O	–	–	–	–	–	–	–	–
Total	49.08	48.94	49.39	51.74	52.17‡	94.48	95.19	89.58
Oxy. atoms	3	3	3	6	6	11	11	14
Si	–	–	–	–	–	3.983	3.942	3.033
Ti	–	–	–	–	–	0.007	0.006	0.007
Al	–	–	–	–	–	0.012	0.085	1.775
Cr	–	–	–	–	–	0.006	0.008	0.096
Fe	0.043	0.056	0.051	0.030	0.038	0.062	0.065	0.265
Mn	0.003	0.003	0.002	0.002	0.002	0.004	0.003	0.009
Mg	0.948	0.935	0.940	0.989	0.975	2.912	2.884	4.813
Ni	–	–	–	–	–	0.017	0.015	0.030
Ca	0.006	0.006	0.007	0.979	0.977	–	–	–
K	–	–	–	–	–	–	–	–
Total	0.999	1.000	0.999	2.000	2.000 ‡	7.003	7.006	10.026
mg# †	0.95	0.93	0.94	0.49	0.49	0.97	0.97	0.94

† Mg/(Fe+Mn+Mg+Ni) ‡ - Total includes 0.44% SrO = 0.008 Sr per 6 Oxygens

* determined by electron-microprobe analysis. The number of analyses is given in brackets. Analytical conditions indicated on Table 2.

minerals, if one assumes that chemical equilibrium was achieved:

$$4Mg_2Si_2O_6 + H_2O + CO_2 = Mg_7Si_8O_{22}(OH)_2 + MgCO_3 \quad (1)$$
enstatite — anthophyllite — magnesite

Table 2 shows that both textural varieties of magnesite have the same chemical composition (101788–1b is the coarse-grained type, and 110488–c2 is the anhedral variety).

Dolomite occurs as fine- to medium-grained, anhedral crystals in textural equilibrium with magnesite; dolomite – magnesite symplectitic intergrowths were observed in two thin sections. Most silicate minerals, including enstatite and anthophyllite, seem to be in stable coexistence with dolomite; however, in several thin sections, dolomite appears to be a product of the replacement of tremolite, suggesting that the following solid-phase reaction proceeded from left to right.

$$Ca_2Mg_5Si_8O_{22}(OH)_2 + 4Mg(CO_3) = 2CaMg(CO_3)_2 + Mg_7Si_8O_{22}(OH)_2 \quad (2)$$
tremolite — magnesite — dolomite — anthophyllite

Olivine has been found in the enstatite – magnesite rock at all but the northernmost occurrence (500 m southeast of 93–43b), which is also the lowest-grade locality. Olivine occurs as texturally late crystals in veinlets that cross-cut and replace enstatite and magnesite (Fig. 4c). At the microscopic scale, the olivine veinlets are not in sharp contact with the surrounding enstatite – magnesite assemblage. Each veinlet has a core of irregular, anhedral olivine that passes transitionally into the enstatite – magnesite rock. In this transition zone, olivine forms pseudomorphs of the original magnesite inclusions in enstatite. The occurrence of olivine in veins suggests that the presence of a fluid phase may have contributed to its formation. The following reaction applies to the coexistence of enstatite, magnesite and olivine in the presence of a fluid phase:

$$Mg_2Si_2O_6 + 2MgCO_3 = 2Mg_2SiO_4 + 2CO_2 \quad (3)$$
enstatite — magnesite — forsterite

Three amphibole minerals, anthophyllite, tremolite and magnesio-cummingtonite, are found in the enstatite – magnesite rock. Anthophyllite replaces enstatite and talc (Fig. 4d), and in some cases overgrows olivine,

TABLE 4. BULK COMPOSITION OF THE FLINTON CREEK METAPERIDOTITES ‡

Sample		110488-c2	1104-c5	103188-c1	110488-c7
Rk. Type		EM	EM	AC	AC
SiO2	wt.%	51.79	39.12	41.38	48.24
TiO2		0.06	0.06	0.01	0.05
Al2O3		1.68	2.07	0.57	1.50
Fe2O3†		10.41	11.54	7.15	9.05
MnO		0.15	0.14	0.11	0.12
MgO		33.19	33.50	32.64	28.45
CaO		0.43	1.64	3.25	4.47
Na2O		0.00	0.24	0.16	0.29
K2O		0.01	0.01	0.10	0.01
P2O5		0.01	0.01	0.01	0.01
S		0.12	0.05	0.09	0.05
Ba	ppm	77	70	61	65
Cr		6255	5156	2091	3333
Zn		109	75	94	101
Ni		2302	1949	1877	1541
V		57	56	20	28
Total		99.11	89.41	86.04	92.98

† Total iron as Fe_2O_3

‡ Analyses made at the University of Ottawa X-ray Fluorescence facility

which also replaces enstatite. It has not been possible to distinguish anthophyllite that developed along the prograde metamorphic path from retrograde anthophyllite that developed at the same time as the anthophyllite – carbonate mantles that surround the enstatite – magnesite rock.

The presence of embayed grains of tremolite in contact with carbonate suggests that tremolite became metastable prior to or during the growth of anthophyllite. Most tremolite crystals have been overgrown by later anthophyllite. Tremolite grains in contact with magnesite are corroded, indicating that prograde metamorphism exceeded the conditions of solid-phase reaction (2) above.

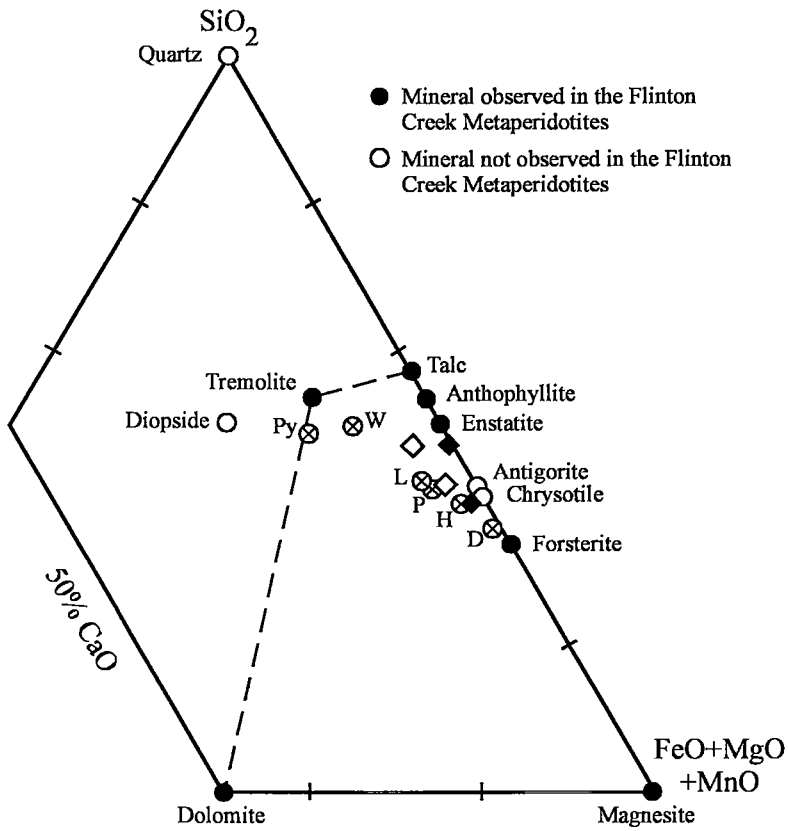

FIG. 3. Minerals commonly observed in metamorphosed ultramafic rocks projected into the system CaO – SiO_2 – (FeO + MgO + MnO). Dark circles indicate minerals observed in the Flinton Creek metaperidotites, unfilled circles designate other minerals commonly associated with metamorphosed ultramafic rocks that were not observed at Flinton Creek. Diagram assumes that a mixed H_2O – CO_2 fluid phase is present in excess. Diamonds indicate the compositions of Flinton Creek metaperidotites listed in Table 2 (open: anthophyllite – magnesite rock, filled: enstatite – magnesite rock). The average compositions of various ultramafic rock-types (Le Maitre 1976) are also shown: Py pyroxenite, W wehrlite, L lherzolite, H harzburgite, D dunite.

Talc is found both as a prograde metamorphic mineral, and as a product of late-stage alteration. Prograde talc occurs as medium- to fine-grained, subhedral laths within enstatite crystals and along enstatite grain-boundaries, indicating the early stability of talc and enstatite. The assemblage talc + enstatite, where not armored in large crystals of enstatite, is usually overgrown by anthophyllite (Fig. 4d). The coexistence of talc + enstatite with anthophyllite is governed by solid-phase reaction (4) below.

$$Mg_3Si_4O_{10}(OH)_2 + 2Mg_2Si_2O_6 = Mg_7Si_8O_{22}(OH)_2 \quad (4)$$
talc enstatite anthophyllite

Petrography of anthophyllite – carbonate rock

This distinctive rock is composed of fine-grained, anhedral carbonate (magnesite and dolomite) and medium-grained, subhedral needles of anthophyllite, which grow in spherical, radiating rosettes with an average radius of approximately 1 cm. Other silicate minerals are present in the anthophyllite – carbonate rock in minor amounts including: magnesio-cummingtonite, chlorite, and late-stage, retrograde talc. No compositional differences could be detected between anthophyllite from the enstatite – magnesite and anthophyllite – carbonate rock types (Table 2).

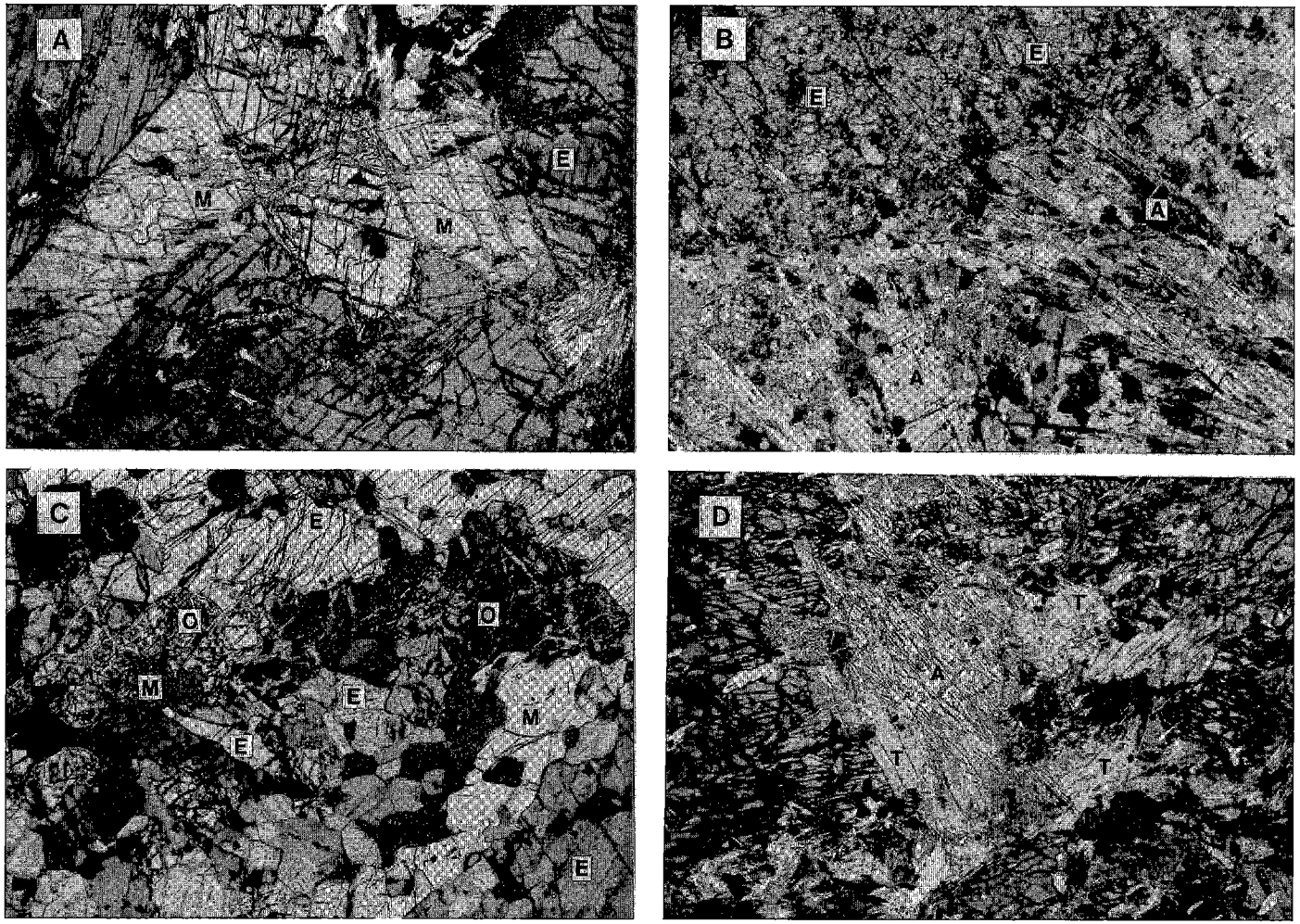

FIG. 4. Photomicrographs of ultramafic assemblages. A. Enstatite – magnesite rock with coarse-grained enstatite (E) and magnesite (M) in textural equilibrium. Width of field: 7 mm. B. Replacement of enstatite (top) by anthophyllite + carbonate. Width of field: 7 mm. C. Late-stage olivine (O) vein running diagonally across center of photo. Olivine has replaced enstatite (E) and magnesite (M), leaving several optically continuous relics of enstatite in center of the photo. Width of field: 3.5 mm. D. Anthophyllite (A) overgrowing talc (T) and enstatite. Width of field: 3.5 mm.

Magnesite and dolomite are more abundant in the anthophyllite – carbonate rock than in the enstatite – magnesite rock, and make up approximately 30 to 50% of the total volume. Magnesite is generally more abundant; however, the ratio of dolomite to magnesite is dependent on proximity of the contact between the ultramafic body and the surrounding host-rock. Although the total amount of carbonate present in the rock remains constant, the proportion of dolomite to magnesite increases outward toward the contact, where dolomite comprises up to 90% of the carbonate present. This relationship suggests that there is a metasomatic control on the amount of dolomite present in the anthophyllite – carbonate rock.

Phase Equilibria Involving Solids In The System $CaO - MgO - SiO_2 - H_2O - CO_2$

The metamorphism of peridotites in the model system $CaO - MgO - SiO_2 - H_2O - CO$ has been described by Greenwood (1967), Johannes (1969), Ohnmacht (1974), Trommsdorff & Evans (1972, 1974, 1977a, b), Evans & Trommsdorff (1970, 1974), and Evans (1977). Phase relations presented in this paper emphasize only those aspects of the model system that apply to the rocks at Flinton Creek. The seven major mineral phases observed in the Flinton Creek ultramafic rocks are shown on Figure 3 in the ternary compositional space $CaO - MgO - SiO_2$. Two additional components, ferrous iron and manganese, are treated as dilutants of the magnesium component. Aluminum occurs primarily in magnesian chlorite, which is always present and does not seem to be involved in reactions with higher- or lower-grade aluminous minerals. Certain minerals observed elsewhere in metamorphosed peridotites do not occur at Flinton Creek; these include quartz, diopside and serpentine.

Three databases contain thermochemical data for all the required phases: Helgeson *et al.* (1978), Berman (1988) and Holland & Powell (1990). The Berman (1988) database can be further subdivided, since it contains two values for magnesite, the first derived by Chernosky & Berman (1989), and a later value obtained by Mäder & Berman (1991). These data are used to examine the equilibrium conditions of the two solid-phase reactions present in the $CaO - MgO - SiO_2 - H_2O - CO_2$ system (reactions 2 and 4 above).

TABLE 5. ACTIVITY MODELS USED FOR CALCULATING EQUILIBRIA

Component	Formula	Activity Model	CA*
Anthophyllite	$Mg_7Si_8O_{22}(OH)_2$	$(X_{Mg})^7$	0.39
Tremolite	$Ca_2Mg_5Si_8O_{22}(OH)_2$	$(3\text{-Ca-K})(X_{Ca})^2(X_{Mg})^5$	0.78
Enstatite	$Mg_2Si_2O_6$	$(X_{Mg})^2$	0.79
Forsterite	Mg_2SiO_4	$(X_{Mg})^2$	0.82
Talc	$Mg_3Si_4O_{10}(OH)_2$	$(X_{Mg})^3$	0.91
Dolomite	$CaMg(CO_3)_2$	(X_{Mg})	0.98
Magnesite	$Mg(CO_3)$	(X_{Mg})	0.94

* Compositions used are the average of those listed in Tables 2 and 3, with the exception of talc, which is from sample 101788-1a only. CA: calculated activity *a*.

The locations of these two equilibria in P – T space have been plotted for the various thermochemical databases using a Microsoft EXCEL spreadsheet program that solves the following equation by iteration:

$$\Delta G^{P,T} = 0 = \Delta H^{Pr,Tr} + \int_{298}^{T} Cp\,dT - T\left[S^{Pr,Tr} + \int_{298}^{T} (Cp/T)\,dT\right] \quad (5)$$
$$+\Delta V^{Pr,Tr}(P-P_r) + (P-P_r)\left[-\Delta v_3 + \Delta v_4 + \Delta v_1(T-T_r) + \Delta v_4(T-T_r)^2\right]$$
$$+(\Delta v_3/2 - \Delta v_4)(P^2-1) + (\Delta v_4/3)(P^3-1) + G_{disorder} + RT\ln K$$

where ΔH, S and ΔV are the enthalpy, entropy and volume of reaction at reference pressure P_r and temperature T_r (1 bar and 298K). Cp is the heat capacity, calculated with the equation of Berman & Brown (1985).

The $\Delta v_1 - \Delta v_4$ terms in equation (5) account for the change in volume of the solid phases with increasing temperature and pressure, using the following expression from Berman (1988):

$$\frac{V_{P,T}}{V_{Pr,Tr}} = 1 + v_1(T-Tr) + v_2(T-Tr)^2 + v_3(P-Pr) + v_4(P-Pr)^2 \quad (6)$$

Note that in equation (5), $\Delta v_1 = \Delta(v_1 \times \upsilon^{Pr,Tr}/10^5)$, $\Delta v_2 = \Delta(v_2 \times \upsilon^{Pr,Tr}/10^5)$, $\Delta v_3 = \Delta(v_3 \times \upsilon^{Pr,Tr}/10^5)$ and $\Delta v_4 = \Delta(v_4 \times \upsilon^{Pr,Tr}/10^8)$, where v_n is the coefficient from equation (6), and υ is the molar volume of each mineral in the reaction at reference temperature, Tr, and pressure, Pr. The Holland & Powell (1990) database can be made compatible with this expression by making the following substitutions for the coefficients of isothermal expansion and compression: $v_1 = \alpha$ and $v_3 = -0.1\ ß$.

The $G_{disorder}$ term was used by Berman (1988) to model progressive disorder in dolomite with increasing temperature from 298.15 K (completely ordered dolomite) to 1423 K (completely disordered). The $G_{disorder}$ term in equation 5 is calculated by:

$$\Delta G_{dis}^{T} = \Delta H_{dis}^{T} - T\Delta S_{dis}^{T} \quad (7)$$

where the ΔH_{dis} and ΔS_{dis} disorder terms are calculated using equations 16 and 17 from Berman (1988), with a slight modification (the newer versions of Berman's database supply d_4 and d_5 terms, which must be substituted for d_3 and d_4 in these earlier equations).

Figure 5 shows the results given by Equation 5 using average measured compositions of the minerals from the Flinton Creek metaperidotites. Activities, given in Table 4, were calculated using an ideal-solution

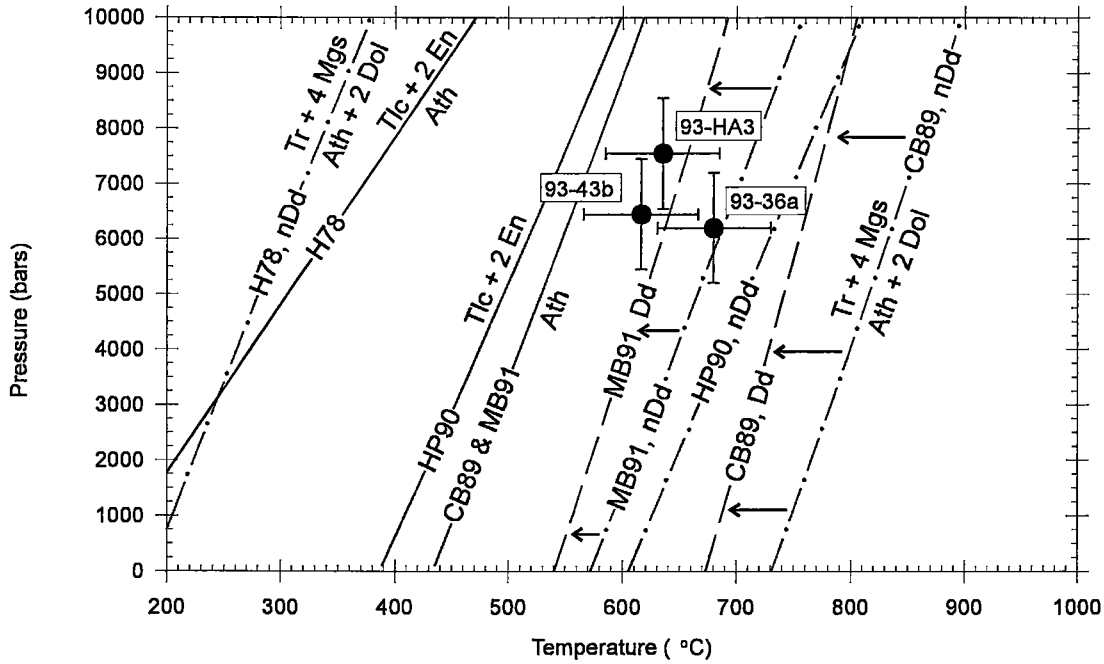

FIG. 5. Calculated solid-phase equilibria in a portion of the system $CaO - SiO_2 - MgO - H_2O - CO_2$ adjusted for the measured compositions of minerals (Tables 2, 3). Solid lines represent the reaction talc + 2 enstatite = anthophyllite. Dashed lines for tremolite + 4 magnesite = anthophyllite + dolomite; Dd indicates that the variable dolomite-disorder model of Berman (1988) was used to the locate the reaction, whereas nDd indicates that the dolomite-disorder model was not used. Thermodynamic datasets used in the calculations are indicated as follows: H78: Helgeson *et al.* (1978), CB89: Chernosky & Berman (1989), HP90: Holland & Powell (1990), MB91: Mäder & Berman (1991). All datasets predict anthophyllite stability for the pressure – temperature range of metamorphism, indicated by black dots with error bars (±50°C, ±1000 bars); the Berman (1988) database, with modified data for magnesite (Mäder & Berman 1991) and variable degree of disorder in dolomite, predicts the stability of anthophyllite + dolomite within error of the estimated P – T range.

model. Also shown in this figure are the thermobarometry results (Table 1), which are considered to represent peak conditions of metamorphism for the Flinton Creek metaperidotites. The observed replacement of talc + enstatite by anthophyllite indicates that the solid-phase equilibrium, reaction (4), limiting the stability of anthophyllite is expected to lie just below the three P – T estimates. The petrographic data also predict the stability of anthophyllite + dolomite relative to tremolite + magnesite for the P – T conditions and mineral compositions at Flinton Creek. Figure 5 demonstrates that the thermodynamic data of Berman (1988), as modified by Mäder & Berman (1991), correspond best with the thermobarometry and petrography of Flinton Creek rocks; this database is used in subsequent calculations.

UNIVARIANT PHASE-RELATIONS

The ultramafic lenses at Flinton Creek are mineralogically similar to the ultramafic boudins at Guglia in the Swiss Alps, as described by Evans & Trommsdorff (1974). At both localities, rocks containing magnesite, talc, enstatite and forsterite are overgrown at some later stage by anthophyllite. Although the two occurrences are mineralogically similar, petrographic analysis reveals substantial differences in the sequence of mineral assemblages that developed.

TABLE 6. FLUID-BEARING ASSEMBLAGES COEXISTING AT INVARIANT POINTS IN THE SYSTEM $MgO-SiO_2$

Absent Phase Designation	Phases Present	
(Ath)	Mgs, En, Fo, Tlc	MEFT*
(En)	Mgs, Ath, Fo, Tlc	MAFT*
(Tlc)	Mgs, Ath, Fo, En	MAFE*
(Fo)	Mgs, Ath, En, Tlc	MATE
(Mgs)	Ath, En, Fo, Tlc	FATE
(Fo, Mgs)	Tlc, En, Ath	TEA

* As designated by Evans & Trommsdorff (1974).

Four mineral phases and a fluid phase form a univariant assemblage in the system $MgO - SiO_2 -$

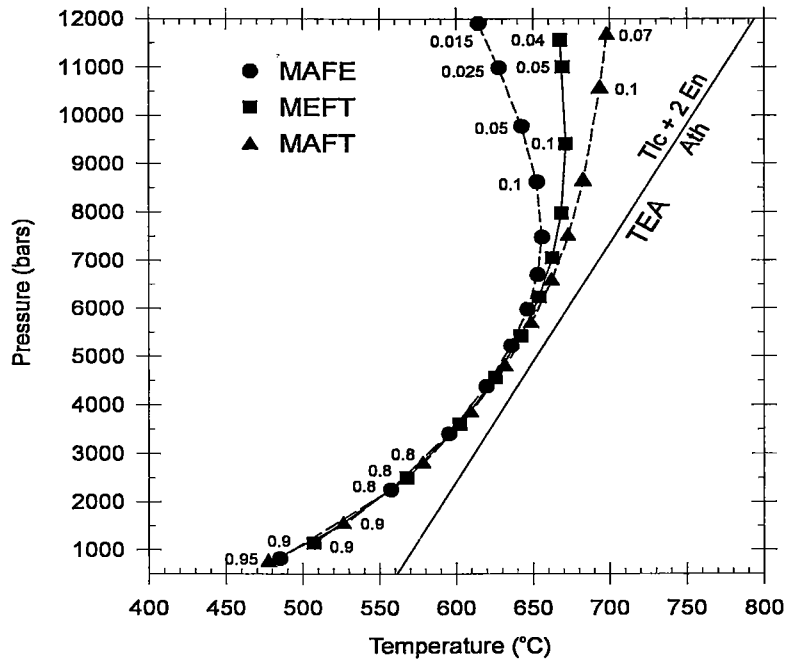

FIG. 6. Pressure – temperature diagram for univariant points with pure magnesian minerals. Symbols along curves and numbers refer to incremental values of the mole fraction of CO_2 along the univariant points. Calculated with database of Berman (1988), as modified by Mäder & Berman (1991). MAFE, MAFT, MEFT, TEA indicate univariant curves with M (magnesite), A (anthophyllite), F (forsterite), E (enstatite), T (talc). Solid curves are stable; dashed curves are metastable.

$H_2O - CO_2$. Evans & Trommsdorff (1974) described one such assemblage characteristic of the univariant condition MEFT (magnesite – enstatite – forsterite – talc – fluid; Table 6), at the Guglia location. The presence of forsterite in the Guglia rocks from the beginning of their petrological evolution is essential to the recognition of the univariant assemblage MEFT as a stable one. This situation contrasts with the rocks at Flinton Creek, where forsterite overprints the earlier magnesite – enstatite assemblage. The significance of these petrographic observations can be understood by locating the various univariant assemblages for the system $MgO - SiO_2 - H_2O - CO_2$ in P – T space. Figure 6 has been calculated with the program TWQ (Berman 1991) using thermodynamic data for end-member magnesian compositions. The figure shows the P–T trajectory of the compositionally degenerate univariant curve, TEA (talc – enstatite – anthophyllite), as well as that of three normal univariant curves, MAFE , MEFT and MAFT. TEA contains both MATE (magnesite – anthophyllite – talc – enstatite) and FATE (forsterite – anthophyllite – talc – enstatite) in P–T space, since both assemblages contain the solid-phase equilibrium, talc + 2 enstatite = anthophyllite. Both MATE and FATE therefore project through the composition dimension onto the P – T path of TEA. TEA and MEFT do not intersect on Figure 6, indicating that the invariant point MEFTA is metastable for end-member magnesian phases using the thermodynamic data of Berman (1988) and Mäder & Berman (1991).

Evans & Trommsdorff (1974) pointed out that the addition of iron to the end-member magnesian phases results in a substantial increase in the field of stability of anthophyllite relative to talc + enstatite, with a corresponding shift in the location of TEA to significantly lower temperatures. According to the database of Berman (1988), the addition of iron causes TEA and the other univariant assemblages indicated on Figure 6 to intersect at a single point (the invariant point MEFTA) for an anthophyllite composition of Ath_{95}; TEA shifts to lower temperatures with further addition of iron, splitting the point MEFTA into duplicate invariant points, as implied on Figure 7 for the measured compositions of the minerals at Flinton Creek, as reported in Tables 3 and 4. For these compositions, the invariant point MEFTA is stable and duplicated at 11,100 bars and <500 bars. MAFT and MAFE are stable between the duplicate invariant

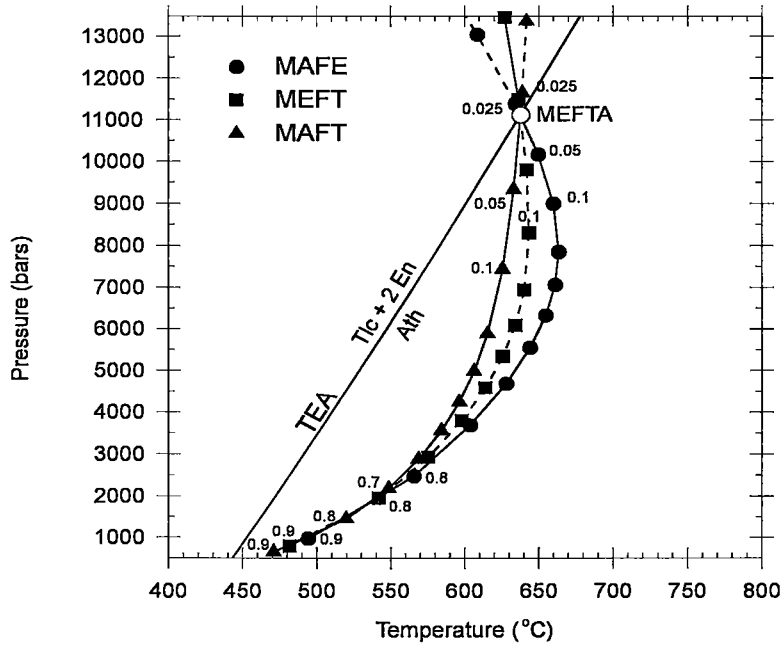

FIG. 7. Pressure – temperature diagram for univariant assemblages, calculated on the basis of measured compositions of the minerals (Tables 2, 3). Number and symbols refer to incremental values of the mole fraction of CO_2 along the univariant curves. Mineral assemblages and thermodynamic data as for Figure 6.

points, and MEFT is stable beyond this range at pressures lower or higher than either of the MEFTA invariant points. It therefore appears that mineral compositions in the Guglia metaperidotites lead to the stability of the MEFT assemblage above the higher-pressure duplicate of the MEFTA invariant point, at approximately 10 kbars.

THE INFLUENCE OF FLUID COMPOSITION

The influence of fluid composition on the mineral assemblage of the ultramafic rocks at Flinton Creek can be examined on Figures 8 and 9, which consider the stability of mineral assemblages, including the calcic phases dolomite and tremolite, on ln fugacity (H_2O) – ln fugacity (CO_2) diagrams, constructed according to the method described by Korzhinskii (1959). The free energy of disordering in dolomite (Berman 1988) has been included in the calculation. Also shown on these figures is the mechanical equilibrium surface along which calculated pressure of fluid is equal to lithostatic pressure $P(CO_2) + P(H_2O) = P_{total}$. This surface was calculated using the nonideal fluid-mixing model of Jacobs & Kerrick (1981). The addition of calcium as a component results in the stability of two additional invariant points labelled DTRAFE and DTRAFT, and listed in Table 7. The fugacity diagrams allow the petrography of the calcic phases to be used as a further check on the evolution of the fluid phase.

TABLE 7. INVARIANT POINTS IN A PORTION OF THE SYSTEM CaO – MgO – SiO_2

Absent Phase	Phases Present	Designation
(Ath, En)	Dol, Fo, Mgs, Tr, Tlc	DTRMFT
(Ath, Mgs)	Dol, En, Fo, Tr, Tlc	DTREFT
(Ath, Fo)	Dol, En, Mgs, Tr, Tlc	DTREMT
(Ath, Tlc)	Dol, En, Fo, Mgs, Tr	DTREMF
(Mgs, Tlc)	Ath, Dol, En, Fo, Tr	DTRAFE
(En, Fo)	Ath, Dol, Mgs, Tr, Tlc	DTRAMT
(En, Mgs)	Ath, Dol, Fo, Tr, Tlc	DTRAFT
(En, Tlc)	Ath, Dol, Fo, Mgs, Tr	DTRAMF
(Fo, Mgs)	Ath, Dol, En, Tlc, Tr	DTRATE
(Fo, Tlc)	Ath, Dol, En, Mgs, Tr	DTRAME

Figure 8 is calculated for 680°C, the thermal maximum applicable to the southern Flinton Synclinorium, as indicated by thermobarometry of rock types other than peridotite. This figure demonstrates that enstatite

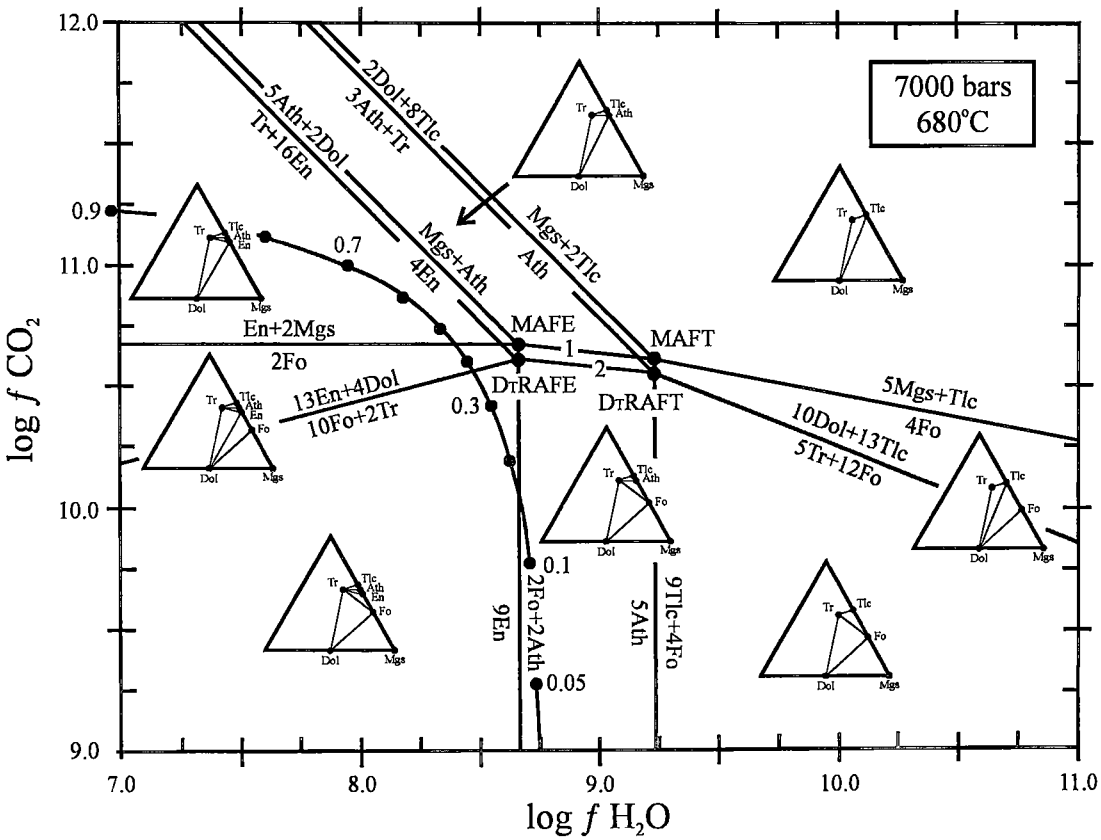

FIG. 8. $\mathrm{Ln}f(H_2O) - \ln f(CO_2)$ diagram at 7000 bars and 680°C. Chemography as shown on Figure 4. The mechanical equilibrium surface, along which fluid partial pressures sum to total pressure, is shown as a curved line, with solid circles and numbers indicating incremental values for the mole fraction of CO_2. Phase relations are indicated for talc (Tlc), anthophyllite (Ath), enstatite (En), forsterite (Fo), magnesite (Mgs), tremolite (Tr), and dolomite (Do). Designations of the invariant points are listed in Tables 6 and 7. Reaction 1: Fo + H_2O + 9CO_2 = Ath + 9Mgs. Reaction 2: 32Fo + 9Tr + 4H_2O + 36CO_2 = 13Ath + 18Dol.

– magnesite assemblages require high $X(CO_2)$ values for stability; this result is in agreement with earlier, lower-pressure (2000 bars) experiments by Greenwood (1967) and Johannes (1969).

Figure 8 provides a possible explanation for the replacement of enstatite – magnesite by late-stage olivine, through the introduction of relatively H_2O-rich fluids [$X(CO_2) < 0.45$] into the enstatite – magnesite rock. Both enstatite and forsterite can be seen on the fugacity diagram to be in equilibrium with dolomite and magnesite, as required by the petrography of the Flinton Creek rocks; enstatite coexists with the carbonates and high-CO_2 fluids along the mechanical equilibrium surface, whereas forsterite and two carbonates coexist with a more H_2O-rich fluid.

Figure 9 is calculated for a temperature of 650°C, corresponding to the development of the anthophyllite – carbonate rock in envelopes that completely replace earlier assemblages in the enstatite – magnesite rock. Decreasing temperature between Figures 8 and 9 reduces the separation between the pairs of invariant points MAFE – DtRAFE and MAFT – DtRAFT such that each pair is almost coincident on Figure 9. The development of the anthophyllite – carbonate assemblage appears to be related to a metasomatic influx of fluid that carries the bulk composition of the peridotite into the stability field of anthophyllite – magnesite. Formation of a metasomatic rind could not have carried on to much lower temperatures, as the mechanical equilibrium surface would intersect the talc – magnesite stability field at approximately 640°C. Talc – magnesite rinds have not been observed surrounding the anthophyllite – carbonate envelope at Flinton Creek.

The stability field of anthophyllite – magnesite – dolomite on Figure 9 is limited along the mechanical equilibrium surface by enstatite – magnesite – dolomite

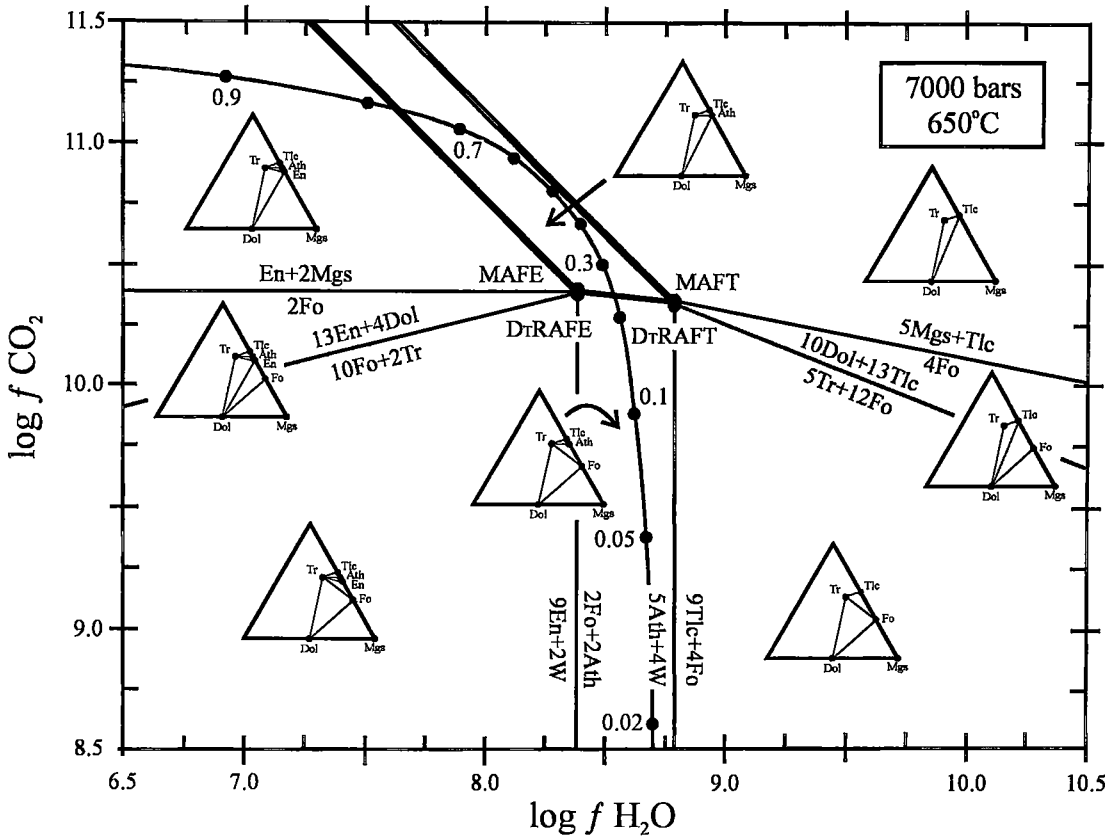

FIG. 9. $Ln(H_2O) - ln f(CO_2)$ diagram at 7000 bars and 650°C. The curved line indicates the location of the mechanical equilibrium surface. Symbols and chemography follow the convention established in Figure 8.

assemblages in CO_2-rich fluids and by forsterite – tremolite assemblages with either dolomite or anthophyllite in H_2O-rich fluids. Beneath the mechanical equilibrium surface, the assemblage anthophyllite – magnesite – dolomite is restricted to fluids that approach binary mixtures of CO_2 and H_2O. For example, the point MAFE occurs at fugacities on Figure 9 corresponding to a $P(CO_2)$ of 2028 bars and a $P(H_2O)$ of 4243 bars, with $P(CO_2) + P(H_2O) = 6271$ bars using the mixing relationships for CO_2 and H_2O from Kerrick & Jacobs (1981); only minor dilution of CO_2 plus H_2O by salts or other gas species is therefore possible with a total fluid pressure of 7000 bars. The metasomatic event that led to the development of anthophyllite – carbonate envelopes around the prograde assemblages apparently took place in the petrological environment represented by Figure 9.

The absence of a talc – magnesite alteration rind, combined with the fact that the mechanical equilibrium surface fails to pass through the anthophyllite + magnesite stability field in Figure 8, indicate that conditions for the formation of the anthophyllite – carbonate rind lie between approximately 650° and 680°C, if one assumes that estimates of metamorphic pressure of 7 kbar ± 1 kbar are correct.

METAMORPHIC EVOLUTION

The metamorphic evolution of the enstatite – magnesite and anthophyllite – carbonate rocks can be summarized using the pressure – temperature and $\log f(H_2O) - \log f(CO_2)$ diagrams in conjunction with available petrographic evidence.

On the basis of existing data, little can be said about the origin of the Flinton Creek metaperidotites prior to their metamorphism in the presence of CO_2-rich fluids and the formation of enstatite – magnesite assemblages. Mineral assemblages such as enstatite + talc and tremolite + magnesite appear to have been stable during the early stages of metamorphism; however, petrographic evidence suggests that they later became metastable relative to anthophyllite and anthophyllite + dolomite. We propose that vein-related, forsterite-bearing assemblages were produced at near-peak

conditions of metamorphism (approximately 680°C), by infiltration of a relatively H_2O-rich fluid along discrete zones, resulting in the local replacement of enstatite – magnesite by forsterite. The anthophyllite – carbonate is considered to have formed during the early stages of cooling (at approximately 650°C) by infiltration of a relatively H_2O-rich fluid phase, resulting in the complete replacement of the enstatite – magnesite assemblage in the smaller ultramafic lenses. Rind formation is believed to have occurred at approximately 650°C because Figure 9 indicates that at this temperature, the anthophyllite – carbonate rind would form from the widest range of compositions of infiltrating fluid without the formation of an additional talc – carbonate rind.

The temperature estimates for the formation of forsterite veins (680°C) and anthophyllite – carbonate rind (650°C) are consistent with those derived from thermobarometry of rocks listed in Table 1. Calculation of additional $\log f(H_2O) - \log f(CO_2)$ diagrams at lower pressures suggests that the temperature estimates for the metamorphism of the ultramafic rocks are relatively independent of the estimated pressure derived from results in Table 1. These consistent estimates of temperature support the suggestion that the ultramafic rocks of the Flinton Creek Complex were metamorphosed simultaneously with the surrounding rocks.

We tentatively conclude that the important factors in accounting for the differences in the petrography of metaperidotites at Flinton Creek and Guglia were higher pressures along the P–T–t path at Guglia and the presence of a CO_2-rich fluid at Flinton Creek.

Conclusions

Ultramafic lenses along 7 kilometers of exposure in the Central Metasedimentary Belt of the Grenville Province were metamorphosed in the presence of a CO_2-rich fluid to produce enstatite – magnesite assemblages as well as accompanying talc, anthophyllite and, ultimately, forsterite. Petrographic evidence indicates the mantle of anthophyllite – magnesite – dolomite rock around cores of the prograde assemblages are the product of a metasomatic process that occurred during retrograde metamorphism in the presence of a fluid phase with a significant content of both CO_2 and H_2O.

Field relationships, including the development of blackwall alteration around the lenses, indicate that metamorphism took place *in situ*. Thermobarometry of adjacent aluminous schists indicates that metamorphic conditions reached at least 680°C and 7000 kilobars.

Acknowledgements

Instruction on the use of the electron microprobe was provided by P. Jones. FDF acknowledges the assistance of an NSERC post-graduate scholarship. The research was supported by a grant to GBS from NSERC. R.M. Easton reviewed an early version of the manuscript and encouraged its submission. Rob Berman, Mike Easton, Robert F. Martin, K. Bucher and an anonymous reviewer provided comment and criticism that considerably improved the manuscript.

References

Berman, R.G. (1988): Internally-consistent thermodynamic data for minerals in the system $Na_2O - K_2O - CaO - MgO - FeO - Fe_2O_3 - Al_2O_3 - SiO_2 - TiO_2 - H_2O - CO_2$. *J. Petrol.* **29**, 445-522.

_____ (1991): Thermobarometry using multi-equilibrium calculations: a new technique, with petrological applications. *Can. Mineral.* **29**, 833-855.

_____ & Brown, T.H. (1985): Heat capacity of minerals in the system $Na_2O - K_2O - CaO - MgO - FeO - Fe_2O_3 - Al_2O_3 - SiO_2 - TiO_2 - H_2O - CO_2$: representation, estimation, and high temperature extrapolation. *Contrib. Mineral. Petrol.* **89**, 168-183.

Bright, E.G. (1986): Geology of the Mellon Lake area. *Ontario Geol. Surv., Open File Rep.* **5598**.

Bucher-Nurminen, K.(1988): Metamorphism of ultramafic rocks in the central Scandinavian Caledonides. *In* Progress in Studies of the Lithosphere in Norway (Y. Kristoffersen, ed.). *Nor. Geol. Unders., Spec. Publ.* **3**, 86-95.

Carmichael, D.M., Moore, J.M. & Skippen, G.B. (1978): Isograds around the Hastings metamorphic "low". *In* Toronto '78 Field Trips Guidebook (A.L. Currie & W.O. Mackasey, eds.). *Geol. Assoc. Can. – Mineral. Assoc. Can.*, 324-346.

Chappell, J.F. (1978): *The Clare River Structure and its Tectonic Setting*. Ph.D. thesis, Carleton Univ., Ottawa, Ontario.

Chernosky, J.V. & Berman, R.G. (1989): Experimental reversal of the equilibrium: clinochlore + 2 magnesite = 3 forsterite + spinel + 2 CO_2 + 4 H_2O and revised thermodynamic properties for magnesite. *Am. J. Sci.* **289**, 249-266.

Evans, B.W. (1977): Metamorphism of alpine peridotite and serpentinite. *Annu. Rev. Earth Planet. Sci.* **5**, 397-447.

_____ & Trommsdorff, V. (1970): Regional metamorphism of ultramafic rocks in the Central Alps: parageneses in the system $CaO - MgO - SiO_2 - H_2O$. *Schweiz. Mineral. Petrogr. Mitt.* **50**, 481-492.

_____ & _____(1974): Stability of enstatite + talc and CO_2-metasomatism of metaperidotite, Val d'Efra, Lepontine Alps. *Am. J. Sci.* **274**, 274-296.

Ford, F.D. & Skippen, G.B. (1994): Shear zone associated, late-stage deformation and retrograde metamorphism on the western margin of the Flinton Synclinorium. *Geol. Assoc. Can. – Mineral. Assoc. Can., Program Abstr.* **19**, A37.

FROST, B.R. (1975): Contact metamorphism of serpentinite, chloritic blackwall and rodingite at Paddy-Go-Easy Pass, central Cascades, Washington. *J. Petrol.* **16**, 272-313.

GREENWOOD, H.J. (1967): Mineral equilibria in the system $MgO - SiO_2 - H_2O - CO_2$. *In* Researches in Geochemistry **2** (P.H. Abelson, ed.). John Wiley, New York, N.Y. (542-567).

HELGESON, H.C., DELANEY, J.M., NESBITT, H.W. & BIRD, D.C. (1978): Summary and critique of the thermodynamic properties of rock forming minerals. *Am. J. Sci.* **278A**, 1-229.

HODGES, K.V. & SPEAR, F.S. (1982): Geothermometry, geobarometry and the Al_2SiO_5 triple point at Mt. Moosilauke, New Hampshire. *Am. Mineral.* **67**, 1118-1134.

HOLLAND, T.J.B. & BLUNDY, J. (1994): Non-ideal interactions in calcic amphiboles and their bearing on amphibole – plagioclase thermometry. *Contrib. Mineral. Petrol.* **116**, 433-447.

_____ & POWELL, R. (1990): An enlarged and updated internally consistent thermodynamic dataset with uncertainties and correlations: the system $K_2O - Na_2O - CaO - MgO - MnO - FeO - Fe_2O_3 - Al_2O_3 - TiO_2 - SiO_2 - C - H_2 - O_2$. *J. Metamorphic Geol.* **8**, 89-124.

JACOBS, G.K. & KERRICK D.M. (1981): APL and FORTRAN programs for a new equation of state for H_2O, CO_2, and their mixtures at supercritical conditions. *Computers and Geoscience* **7**, 131-143.

JAHNS, R.H. (1967): Serpentinites of the Roxbury district, Vermont. *In* Ultramafic and Related Rocks (P.J. Wyllie, ed.). John Wiley, New York, N.Y. (137-160).

JOHANNES, W. (1969): An experimental investigation of the system $MgO - SiO_2 - H_2O - CO_2$. *Am. J. Sci.* **267**, 1083-1104.

KENDEL, F. (1970): CO_2-Metasomatose in Peridotiten des Aaheimer Gebietes (W-Norwegen). *Fortschr. Mineral.* **48**(1), 13-14.

KERRICK, D.M. & JACOBS, G.K. (1981): A modified Redlich – Kwong equation for H_2O, CO_2 and $H_2O - CO_2$ mixtures at elevated pressures and temperatures. *Am. J. Sci.* **281**, 735-767.

KOHN, M.J. & SPEAR, F.S. (1990): Two new geobarometers for garnet amphibolites, with applications to southeastern Vermont. *Am. Mineral.* **75**, 89-96.

KORZHINSKII, D.S. (1959): *Physicochemical Basis of the Analysis of the Paragenesis of Minerals.* Consultants Bureau Inc., New York, N.Y.

LE MAITRE, R.W. (1976): The chemical variability of some common igneous rocks. *J. Petrol.* **17**, 589-637.

MÄDER, U.K. & BERMAN, R.G. (1991): An equation of state for carbon dioxide to high pressure and temperature. *Am. Mineral.* **76**, 1547-1559.

OHNMACHT, W. (1974): Petrogenesis of carbonate-orthopyroxenites (sagvandites) and related rocks from Troms, northern Norway. *J. Petrol.* **15**, 303-323.

PETTERSEN, K. (1883): Sagvandit, en ny bergart. *Tromsö Mus. Arsh.* **6**, 81.

POWELL, R. & HOLLAND, T. (1990): Calculated mineral equilibria in the pelite system, KFMASH ($K_2O - FeO - MgO - Al_2O_3 - SiO_2 - H_2O$). *Am. Mineral.* **75**, 367-380.

PRINGLE, G.J. (1989): EDDI – a FORTRAN computer program to produce corrected microprobe analyses of minerals using an energy dispersive X-ray spectrometer. *Geol. Surv. Can., Open File Rep.* **2127**.

SANFORD, R.F. (1982): Growth of ultramafic reaction zones in greenschist to amphibolite facies metamorphism. *Am. J. Sci.* **282**, 543-616.

SCHREYER, W., OHNMACHT, W. & MANNCHEN, J. (1972): Carbonate-orthopyroxenites (sagvandites) from Troms, northern Norway. *Lithos* **5**, 345-364.

THOMPSON, J.B., JR. (1959): Local equilibrium in metasomatic processes. *In* Researches in Geochemistry **1** (P.H. Abelson, ed.). John Wiley, New York, N.Y. (427-457).

THOMPSON, P.H. (1972): *Stratigraphy, Structure and Metamorphism of the Flinton Group in the Bishop Corners – Madoc Area, Grenville Province, Eastern Ontario.* Ph.D. thesis, Carleton Univ., Ottawa, Ontario.

_____ (1973): Mineral zones and isograds in "impure" calcareous rocks, an alternative means of evaluating metamorphic grade. *Contrib. Mineral. Petrol.* **42**, 63-80.

TROMMSDORFF, V. & EVANS, B.W. (1972): Progressive metamorphism of antigorite schist in the Bergell tonalite aureole (Italy). *Am. J. Sci.* **272**, 423-437.

_____ & _____ (1974): Alpine metamorphism of peridotitic rocks. *Schweiz. Mineral. Petrogr. Mitt.* **54**, 333-352.

_____ & _____ (1977a): Antigorite-ophicarbonates: phase relations in a portion of the system $CaO - MgO - SiO_2 - H_2O - CO_2$. *Contrib. Mineral. Petrol.* **60**, 39-56.

_____ & _____ (1977b): Antigorite-ophicarbonates: contact metamorphism in Valmalenco, Italy. *Contrib. Mineral. Petrol.* **62**, 301-312.

WYNNE-EDWARDS, H.R. (1972): The Grenville Province. *In* Variations in Tectonic Styles in Canada (R.A. Price & R.J.W. Douglas, eds.). *Geol. Assoc. Can., Spec. Pap.* **11**, 263-334.

Received March 23, 1996, revised manuscript accepted June 16, 1997.